Pharm Res (2019) 36: 168
https://doi.org/10.1007/s11095-019-2688-2

RESEARCH PAPER

Transferrin Receptor Targeted Cellular Delivery of Doxorubicin Via a Reduction-Responsive Peptide-Drug Conjugate

Songtao Li[1] • Hongling Zhao[1] • Xiaoxia Mao[1] • Yanfang Fan[2] • Xiujun Liang[2] • Ruxing Wang[1] • Lijun Xiao[3] • Jianping Wang[3] • Qi Liu[1] • Guiqin Zhao[1]

Received: 5 June 2019 / Accepted: 15 August 2019 / Published online: 25 October 2019

ABSTRACT

Purpose Transferrin receptors (TfRs) are overexpressed in tumor cells but are scarce in normal tissues, which makes TfR an attractive target for drug treatment of cancer. The objective of this study was to evaluate the potential of BP9a (CAHLHNRS) as a peptide vector for constructing TfR targeted peptide-drug conjugates and selective drug delivery.

Methods Doxorubicin (DOX) was connected to BP9a via a disulfide-intercalating linker to afford a reduction-responsive BP9a-SS-DOX conjugate. By using HepG2 human liver cancer cells and L-O2 normal hepatic cells as TfR over-expressing and low-expressing *in vitro* models, respectively, TfR mediated cellular uptake of this conjugate was studied by using flow cytometry and confocal laser scanning microscopy. The *in vitro* cytotoxicities of the conjugate against HepG2 and L-O2 cells were examined by cell counting kit-8 (CCK-8) assay to evaluate its tumorous specificity.

Results Cellular uptake and TfR blockage test results showed that the BP9a-SS-DOX conjugate gained entry into HepG2 cells via endocytosis mediated by TfR and mainly accumulated in cytoplasm. The *in vitro* antiproliferative activity of this conjugate against HepG2 cells (IC_{50} 6.21 ± 1.12 μM) was approximately one-sixth of that of free DOX (IC_{50} 1.03 ± 0.13 μM). However, its cytotoxic effect on L-O2 cells was obviously reduced compared with that of free DOX.

Conclusions The BP9a-SS-DOX conjugate showed specific antiproliferative activity against HepG2 liver cancer cells. Our study suggests that BP9a has the potential to target chemotherapeutic agents to tumor cells over-expressing TfR and facilitate selective drug delivery.

KEY WORDS peptide-doxorubicin conjugate · reduction-responsive · targeted drug delivery · transferrin receptor · tumor specificity

ABBREVIATIONS

CCK-8	Cell counting kit-8
CTC	Chlorotrityl chloride
DAPI	4′, 6-diamidino-2-phenylindole
DIC	N, N′-diisopropylcarbodiimide
DIPEA	N, N-diisopropylethylamine
DMF	N, N-dimethylformamide
DMSO	Dimethyl sulfoxide
DOX	Doxorubicin
EDT	1, 2-ethanedithiol
EGFP	Enhanced green fluorescence protein
ESI MS	Electrospray ionization mass spectrometry
Fmoc	9-fluorenylmethoxycarbonyl
HOBt	1-hydroxybenzotriazole
MFI	Mean fluorescence intensity
RP-HPLC	Reversed-phase high-performance liquid chromatography
SPDP	3-(2-pyridyldithio) propionic acid N-hydroxysuccinimide ester
TEA	Triethylamine
TFA	Trifluoroacetic acid
TfR	Transferrin receptor

✉ Songtao Li
songtao-li@hotmail.com

✉ Guiqin Zhao
zgq164190162@163.com

[1] Hebei Province Key Laboratory of Research and Development of Traditional Chinese Medicine, Institute of Chinese Mateia Medica Chengde Medical University Chengde 067000, China

[2] Institute of Basic Medicine, Chengde Medical University Chengde 067000, China

[3] Department of Immunology, Chengde Medical University Chengde 067000, China

TIS Triisopropylsilane
TLC Thin-layer chromatography

INTRODUCTION

The clinical application of doxorubicin (DOX) has been restricted by severe side effects caused by its nonspecific toxicity to noncancerous tissues. Linking cytotoxic agents to targeted ligands which have high binding affinity toward receptors overexpressed on the surface of tumor cell has been considered as an effective strategy to improve the specificity of drugs to tumor tissues (1–4). Transferrin receptor (TfR), which belongs to type II transmembrane glycoprotein (5,6), has a special extracellular structure and can mediate the endocytosis of transferrin (Tf), so it is identified as an important regulatory protein involving iron balance and cell growth regulation (7). Overexpression of TfR in tumor cells (8–13) but not in normal tissues makes it possible to use TfR specific binding ligands as targeted vectors for selective drug delivery (14–24), which may help to enhance the uptake of drugs by tumor cells and reduce toxic effect on normal cells. DOX-Tf conjugate has been studied extensively as a TfR targeted drug-protein complex for selective and enhanced drug delivery (25). Despite the promising results obtained in previous studies, the application of Tf as the drug carrier is restricted due to the high concentration of endogenous Tf in blood. The native Tf can exert a competitive inhibition on Tf-drug conjugates, which may weaken their *in vivo* TfR targeting potency (24). Moreover, the high molecular weight of Tf makes it difficult to use this protein ligand for constructing drug delivery systems (26).

Peptides are considered as a novel class of tumor targeted vectors following after proteins including antibodies. As tumor targeted drug carriers, peptides may have the advantages of being relatively easy to synthesize in large scale and conjugate with drugs, possessing higher tissue penetration capacity and lower immunogenicity in comparison with proteins (27,28). Additionally, the number and regioselectivity of the conjugated drug molecules on a peptide are controllable, which is difficult for protein (1). Phage display technology is one of the most important methods to acquire tumor targeted binding peptides (28,29). Zheng and colleagues screened TfR affinity phage clones from 7-mer phage display library and discovered a peptide BP9 (AHLHNRS) which showed high affinity to TfR (30). They expressed a fusion protein by combining enhanced green fluorescence protein (EGFP) with BP9 in *E. coli*, and fluorescence microscopy results showed that the EGFP-BP9 protein could bind to liver cancer cells over-expressing TfR. This research group further used BP9 as a TfR targeted peptide to fused with curcin, a protein which has antiproliferative activity but no selectivity, to afford a novel recombinant protein curcin-TfRBP9 (31). Immunofluorescence analysis results indicated that BP9 enabled curcin to selectively bind to and enter into human liver cancer HepG2 cells over-expressing TfR, and the recombinant protein mainly located in the cytoplasm of HepG2 cells. Nevertheless, less or no fluorescence signal was detected in L-O2 normal hepatic cells expressing low level of TfR. The curcin-TfRBP9 fusion protein exhibited higher antiproliferative activity against HepG2 cells than curcin, and its cytotoxic effect on L-O2 cells was much lower when compared with that of HepG2 cells. These results suggested that peptide BP9 remarkably enhanced the targeting efficacy of curcin on tumor cells over-expressing TfR.

Tumor targeted reduction-responsive drug delivery systems have received considerable attention due to their site-specific and effective drug release characteristics. Reduction-responsive drug delivery systems generally contain an intramolecular disulfide bond between drugs and the carrier, which can be effectively cleaved by reduced glutathione (GSH) but maintain stable under normal conditions. It has been revealed that the intracellular GSH concentration is 1000 times higher than that in blood circulation (32,33). In addition, tumor tissues were found to contain several times higher concentrations of GSH as compared with normal tissues (34), these differential GSH concentration levels make reduction-responsive drug delivery systems more rapidly release drugs under the reductive microenvironment within tumor cells (35–39).

In order to enlarge the application of BP9 as a TfR targeted peptide vehicle to connect with cytotoxic molecules by chemical synthesis method, we previously designed and synthesized a N-terminus cysteine modified BP9 analog (BP9a, CAHLHNRS) (40). In this study, DOX was connected with BP9a through 3-(2-pyridyldithio) propionic acid N-hydroxysuccinimide ester (SPDP) as a reducible linker to afford a reduction-responsive peptide-drug conjugate (BP9a-SS-DOX). The *in vitro* drug release character of this conjugate was determined by co-incubation with GSH solution at different concentrations. The cellular uptake and intracellular localization of the BP9a-SS-DOX conjugate in HepG2 and L-O2 cells were investigated by flow cytometry and confocal laser scanning microscopy. The cytotoxic effects of this peptide-drug conjugate on HepG2 and L-O2 cells, respectively, were examined using cell counting kit-8 (CCK-8) assay to evaluate its specificity.

MATERIALS AND METHODS

Materials

Doxorubicin hydrochloride (DOX·HCl) was purchased from Aladdin Biochemical Technology Co., Ltd. (Shanghai, China); SPDP and Trifluoroacetic acid (TFA) were obtained from J&K Scientific Ltd. (Beijing, China); 2-chlorotrityl chloride (2-CTC) resin was supplied from NanKai HeCheng Co., Ltd. (1.3 mmol/g capacity, G55120103–1, Tianjin, China); GSH and Dimethyl sulfoxide (DMSO) were purchased from Sigma; CCK-8 was obtained from MedChemExpress (NJ, USA); 4′, 6-

diamidino-2-phenylindole (DAPI) solution was purchased from Solarbio Life Sciences & Technology Co., Ltd. (Beijing, China); The reagents, N, N′-diisopropylcarbodiimide (DIC), 1-hydroxybenzotriazole (HOBt), Triethylamine (TEA), N, N-diisopropylethylamine (DIPEA) were purchased from Highfine Biotech Co., Ltd. (Jiangsu, China); All of the 9-fluorenylmethoxycarbonyl (Fmoc)-protected amino acids were obtained from Chengnuo New Technology Co., Ltd. (Chengdu, China), including Fmoc-Ser(tBu)-OH, Fmoc-Arg(Pbf)-OH, Fmoc-Asn(Trt)-OH, Fmoc-His(Trt)-OH, Fmoc-Leu-OH, Fmoc-Ala-OH and Fmoc-Cys(Trt)-OH. Acetonitrile (CH_3CN) and Methanol (MeOH) for reversed-phase high-performance liquid chromatography (RP-HPLC) were of chromatographic grade and obtained from Starmark Science and Technology Development Co., Ltd. (Tianjin, China); All other reagents and solvents were of analytical grade and used without further purification.

Synthesis of DOX-SS-Pyr

DOX-SS-Pyr was synthesized according to the published procedures (41,42) with minor modification. Briefly, to the mixture of DOX·HCl (17.4 mg, 30 μmol) and SPDP (11.2 mg, 36 μmol) in DMSO (5 mL) was added dropwise TEA (6.25 μL, 45 μmol). The reaction mixture was stirred at 50°C and the progress of the reaction was monitored by thin-layer chromatography (TLC) with dichloromethane: methanol (13: 1, v: v) as developing solvents. After stirred for 6 h, the product of DOX-SS-Pyr was purified by column chromatography on silica gels (dichloromethane: methanol = 20: 1, v: v) and characterized by analytical RP-HPLC, ESI MS and ^{1}H NMR spectra.

Synthesis of BP9a

BP9a was synthesized manually on 2-CTC resin (1.3 mmol/g capacity) using Fmoc-chemistry as described earlier (40). Briefly, the Fmoc-Ser(tBu)-OH (5.78 g, 15 mmol) was coupled to 2-CTC (3.85 g, 5 mmol) resin *in situ* using DIPEA (3 mL, 15 mmol) in DMF. After Fmoc deprotection by 20% piperidine in DMF, Fmoc-Arg(Pbf)-OH (9.65 g, 15 mmol) was coupled to the amino group of serine by using DIC (3.5 mL, 22.5 mmol) and HOBt (3.05 g, 22.5 mmol) as coupling reagents in DMF for 2 h. The synthesis of the peptide was continued by repeating the Fmoc deprotection and coupling processes according to the peptide sequence from C to N terminus. The peptide was cleaved from the resin by stirring of the fully protected peptide resin in a mixture of TFA: 1, 2-ethanedithiol (EDT): H_2O: Triisopropylsilane (TIS) (94: 2.5: 2.5: 1, v: v) at room temperature for 2 h, and the cleavage mixture was filtered to remove the resin. Then the filtrate was precipitated and washed with ice-cold diethyl ether four times. The crude peptide was purified by semi-preparative RP-HPLC, lyophilized and characterized by analytical RP-HPLC and ESI MS.

Synthesis of the BP9a-SS-DOX Conjugate

The BP9a-SS-DOX conjugate was prepared through thiol-disulfide exchange reaction. Briefly, to a solution of BP9a (14.1 mg, 15 μmol) in anhydrous DMF (2 mL) was added a solution of DOX-SS-Pyr (13.3 mg, 18 μmol) dissolved in anhydrous DMF (3 mL). The reaction mixture was stirred under nitrogen atmosphere at room temperature overnight and then precipitated and washed with ice-cold diethyl ether four times. The resulting BP9a-SS-DOX conjugate was purified by semi-preparative RP-HPLC and characterized by analytical RP-HPLC and ESI MS.

RP-HPLC

Analytical RP-HPLC was performed on a Thermo U3000 liquid chromatograph (Thermo Fisher, US) equipped with an Innoval C18 column (250 mm × 4.6 mm, 5 μm). Analysis was achieved using a linear gradient of 5–95% eluent B (eluent A: 0.1% TFA in H_2O; eluent B: (0.1% TFA in CH_3CN-H_2O (90:10, v:v)) for 20 min at a flow rate of 1 mL/min, and absorbance detected at 215 nm.

Final purification of the crude products was carried out using RP-HPLC on a semi-preparative Hedera ODS-2 C18 column (250 mm × 10 mm, 10 μm) with a linear gradient of 10–20% or 20–40% eluent B (eluent A: 1% TFA in H_2O; eluent B: CH_3CN) over 30 min. The flow rate was 8 mL/min and peaks were detected at 215 nm.

Mass Spectrometry

ESI MS analysis was carried out with an Agilent 6420 Triple Quadrupole LC/MS system (Agilent Technologies, USA). Analyses were conducted in positive ion mode, and the operating parameters were set as follows: capillary voltage, 4.0 kV; drying gas flow rate, 10 L/min; drying gas temperature, 330°C; nebulizer pressure, 35 psi.

In Vitro Drug Release

The BP9a-SS-DOX conjugate was initially dissolved in DMSO (10 μL), then a solution of GSH dissolved in PBS (5 mM or 5 μM concentration) was added to a final volume of 1 mL (final concentration of the BP9a-SS-DOX conjugate was 100 μM). The mixtures were incubated at 37°C and 100 μL aliquots were taken out at 0, 0.5, 1, 2, 4, 8 and 24 h, respectively. The sample solution at each selected time point was analyzed by using RP-HPLC, and the ratio for each BP9a-SS-DOX conjugate remained intact was examined by comparing the peak areas detected by RP-HPLC before and after treatment with GSH.

Cell Lines

Human HepG2 liver cancer cells obtained from the Cell Resource Center of Peking Union Medical College (Beijing, China) were cultured in DMEM (Gibco) containing 10% fetal bovine serum (Gibco) and 1% penicillin/streptomycin. Human L-O2 normal hepatic cells, which were kindly provided by Professor Mingyu Gong at the Department of Biochemistry, Chengde Medical University, were grown in RPMI-1640 (Gibco) containing 10% fetal bovine serum (Gibco) and 1% penicillin/streptomycin. Cell cultures were maintained at 37°C in a humidified atmosphere with 5% CO_2.

Cellular Uptake Studies

Flow cytometry was used to investigate the cellular uptake of free DOX or the BP9a-SS-DOX conjugate by HepG2 cells over-expressing TfR and L-O2 cells with lack of TfR, respectively. 2.5×10^5 cells/well were seeded into 6-well plates and were cultured at 37°C for 24 h. Cells were then treated with free DOX or the BP9a-SS-DOX conjugate (equivalent DOX concentration of 5 μM) for 3 h. After removing the drug solution and washing the cells twice with PBS, the cells were detached by adding trypsin and then centrifuged at 2000 rpm for 10 min. The precipitated cells were washed twice with PBS, suspended with PBS and analyzed using a flow cytometer (BD FACSCalibur, USA). The number of cells collected for analysis was 1×10^4.

The cellular uptake and intracellular distribution of free DOX or the BP9a-SS-DOX conjugate were also directly observed by confocal laser scanning microscopy. Briefly, HepG2 or L-O2 cells were seeded on glass coverslips that were placed in 6-well plates at a density of 5×10^4 cells/well. After cultured at 37°C for 24 h, cells were treated with free DOX or the BP9a-SS-DOX conjugate (equivalent DOX concentration of 5 μM) and incubated for 3 h at 37°C. Following removal of the drugs, cells were washed twice with PBS and fixed with 4% paraformaldehyde for 30 min. Cell nuclei staining was performed with DAPI for 10 min according to the procedure of manufacturer. Then the fluorescent images of cells were analyzed using a confocal laser scanning microscope (Nikon Eclipse C1Si, Japan). The excitation/emission wavelengths were set at 350/460 nm (blue) and 480/580 nm (red), respectively, for detecting the fluorescence produced by DAPI and DOX.

TfR Competitive Inhibition Assay

A TfR competitive inhibition assay was conducted on HepG2 cells to further investigate the cellular uptake pathway of the BP9a-SS-DOX conjugate. The cells seeded into 6-well plates or on glass coverslips in 6-well plates were preincubated with serum free cultural medium containing BP9 (20 μM) at 37°C for 2 h. After the BP9 solution was removed, cells were washed twice with PBS and then treated with the BP9a-SS-DOX conjugate (equivalent DOX concentration of 5 μM) at 37°C for 3 h. Cellular uptake was analyzed by flow cytometry and confocal microscopy.

In Vitro Cytotoxicity

CCK-8 assay was used to evaluate *in vitro* cytotoxic effects of free DOX or the BP9a-SS-DOX conjugate on HepG2 and L-O2 cells, respectively. Cells were seeded in 96-well cell-culture plates (5×10^3 cells/well) in 100 μL of complete culture medium and incubated at 37°C in a 5% CO_2 atmosphere for 24 h. The medium was then replaced with serial diluted solutions of free DOX or the BP9a-SS-DOX conjugate. After incubation for 48 h, CCK-8 (10 μL) was added to each well and incubated for a further 3 h at 37°C. Cells without drug treatment were used as the control. The absorbance at 450 nm for each well was measured on a microplate reader (Bio Tek, Elx808).

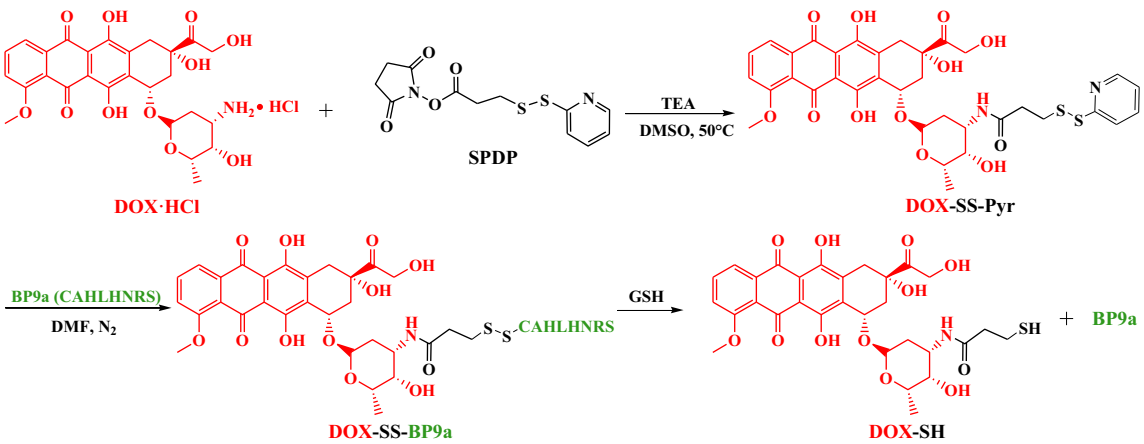

Scheme 1 Synthetic route and drug release of the BP9a-SS-DOX conjugate.

Statistical Analysis

Data were expressed as the mean ± standard deviation, and statistical analysis was performed using an unpaired Student's t test. Data were considered significantly different at $P < 0.05$, $P < 0.01$ and $P < 0.001$.

RESULTS AND DISCUSSION

Synthesis and Drug Release Study of the BP9a-SS-DOX Conjugate

There are three modification sites in the structure of DOX: amidogen at the sugar group, C-13 carbonyl and C-14 hydroxyl. The amidogen can react with N-hydroxysuccinimide ester of some crosslinkers to form an amido bond (41,43,44); C-13 carbonyl generally reacts with hydrazine of crosslinkers to form a pH sensitive hydrazone bond which can release free DOX under acidic condition (45–47); and C-14 hydroxyl was used to conjugate with tumor targeted peptides via anhydrides (48–50). SPDP is a commonly used heterobifunctional crosslinker for constructing reduction-responsive drug delivery systems because the 3-(2-pyridyldithio) and N-hydroxysuccinimide ester functional groups of SPDP can react with sulfydryl of peptide vectors and amidogen of chemotherapeutic agents, respectively. In the present study, we chose SPDP as the crosslinker to connect DOX with BP9a to afford a reduction-responsive peptide-drug conjugate (BP9a-SS-DOX). The synthetic route of the BP9a-SS-DOX conjugate is depicted in Scheme 1. Firstly, under the action of a catalytic amount of TEA, the 3′ amino group of DOX was reacted with the N-hydroxysuccinimide ester of SPDP to generate DOX-SS-Pyr, which was identified by analytical RP-HPLC (95.7% purity), ESI MS m/z, $[M + H]^+$ 741.5 (calculated), 741.3 (observed) and ^1H NMR spectra (400 MHz, DMSO-d6) which was consistent with literature (38); Secondly, Fmoc/tBu solid phase strategy was used for the synthesis of BP9a and its total yield was 39.4%. The peptide was purified to 98.4% purity by semi-preparative RP-HPLC, and its molecular weight value was identified by ESI MS m/z, $[M + H]^+$ 938.2 (calculated), 937.6 (observed); Finally, the 2-pyridyldithio group of DOX-SS-Pyr reacted with the sulfydryl of BP9a via thiol-disulfide exchange reaction to give the BP9a-SS-DOX conjugate as a deep red powder. The product was purified by semi-preparative RP-HPLC and was validated by analytical RP-HPLC (97.6% purity) and ESI MS m/z, $[M + H]^+$ 1566.7 (calculated), 1566.8 (observed); $[M + 2H]^{2+}$ 783.8 (calculated), 784.1 (observed).

The *in vitro* drug release profile of the BP9a-SS-DOX conjugate (Fig. 1) showed that the disulfide bond between BP9a and DOX could be efficiently cleaved by being co-incubated with 5 mM GSH solution because only 2.4% of the BP9a-SS-DOX conjugate remained intact after incubation for 24 h, indicating that over 97% of DOX-SH was released from the conjugate. However, cleavage of the disulfide bond was much slower when the conjugate was co-incubated with 5 μM GSH solution, causing less than 25% of DOX-SH to be released from the conjugate after 24 h incubation.

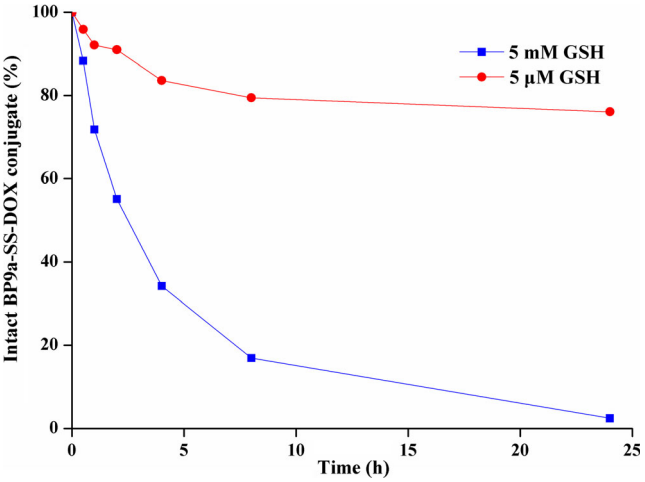

Fig. 1 *In vitro* drug release of DOX-SH from the BP9a-SS-DOX conjugate after co-incubation with 5 mM or 5 μM GSH solution.

In Vitro Cellular Uptake Study

Flow cytometry was used to quantify the intracellular accumulation of free DOX or the BP9a-SS-DOX conjugate in HepG2 liver cancer cells over-expressing TfR and L-O2 hepatic cells expressing low level of TfR. As shown in Fig. 2, there was little difference in the intracellular fluorescence intensity of DOX in both cell lines (mean fluorescence intensity, MFI 721.71 for HepG2 cells and 772.06 for L-O2 cells, respectively) after treatment with free DOX for 3 h, whereas the intracellular fluorescence intensity of DOX produced from the BP9a-SS-DOX conjugate in HepG2 cells (MFI 278.44, Fig. 2a) was higher than that in L-O2 cells (MFI 58.43, Fig. 2b) when cells were incubated with the conjugate for 3 h, indicating that the specific cellular uptake of the BP9a-SS-DOX conjugate by cells expressing higher level of TfR.

The intracellular localizations of free DOX or the BP9a-SS-DOX conjugate in HepG2 and L-O2 cells, respectively, were directly observed by using laser confocal scanning microscopy, and the results were shown in Fig. 3. The autofluorescence of DOX was displayed in red, and the cellular nuclei were stained with DAPI which can be detected with blue fluorescence. Both of the two drugs could enter into HepG2 cells but they exhibited different intracellular distributions. The red fluorescence of DOX accumulated largely in the nuclei of HepG2 cells treated with free DOX, whereas for HepG2 cells treated with the BP9a-SS-DOX conjugate, the accumulation of the peptide-drug conjugate was mainly located in

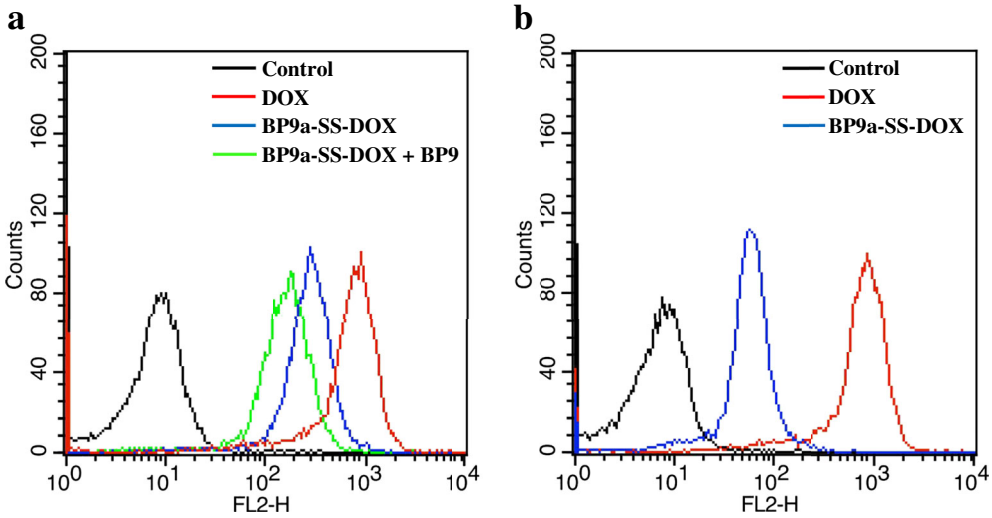

Fig. 2 Cellular uptakes of free DOX or the BP9a-SS-DOX conjugate by HepG2 (**a**) and L-O2 (**b**) cells after 3 h incubation were analyzed by using flow cytometry. For TfR competitive inhibition assay, HepG2 cells were preincubated with BP9 for 2 h and then treated with the BP9a-SS-DOX conjugate. The black, red, blue and green line represent control, DOX, BP9a-SS-DOX alone and BP9a-SS-DOX with BP9 pretreatment, respectively.

cytoplasm and perinuclear region (Fig. 3a). These results suggested that the BP9a-SS-DOX conjugate might have a different uptake pathway by HepG2 cells from that of free DOX. Figure 3b showed that the red fluorescence of DOX also located in the nuclei of L-O2 cells treated with free DOX, indicating that free DOX can permeate into L-O2 cells and has no selectivity between tumor and normal cells. While for L-O2 cells treated with the BP9a-SS-DOX conjugate, the red fluorescence of DOX was barely visible as shown in Fig. 3b, illustrating that by connecting with TfR targeted binding peptide BP9, DOX could not efficiently enter into L-O2 cells as its free form. This might be related to the scarce TfR expression on the surface of L-O2 cells. On the basis of these results, we hypothesized that cellular uptake of the BP9a-SS-DOX conjugate by HepG2 cells could possibly be via overexpressed TfR present there.

TfR Competitive Inhibition Assay

BP9 was found to have high binding affinity towards TfR, which may help to block the binding sites of TfR to the BP9a-SS-DOX conjugate and inhibit its cellular uptake. To further verify whether the cellular uptake of the BP9a-SS-DOX conjugate was dependent on the endocytosis mediated by targeted binding of BP9a towards TfR, a TfR inhibition test was carried out through competitive blockade of TfR with BP9 and the result was analyzed by means of flow cytometry and confocal microscopy. As shown in Fig. 2a, for HepG2 cells which were pretreated with excess BP9 for 2 h, the MFI value of DOX produced from the BP9a-SS-DOX conjugate (163.46) was obviously decreased in comparison with that (278.44) of cells without pretreatment with BP9. Also, Fig. 3a showed that the red fluorescence intensity of DOX produced from the BP9a-SS-DOX conjugate was clearly reduced in the case of HepG2 cells pretreated with BP9 compared with that of cells without preincubation with BP9. These results indicated that when TfR was blocked by BP9, the targeted effect of the BP9a-SS-DOX conjugate was weakened, suggesting that the entry of this conjugate into HepG2 cells was related to the endocytosis mediated by TfR overexpressed on the surface of cells.

In Vitro Cytotoxicity

To evaluate the antiproliferative activity and selective cytotoxicity of the BP9a-SS-DOX conjugate, HepG2 liver cancer cell line and L-O2 hepatic cell line were chosen based on their different TfR expressing levels. The antiproliferative activities of free DOX and the BP9a-SS-DOX conjugate against HepG2 cells, and the cytotoxic effects of these two drugs on L-O2 cells were evaluated by using CCK-8 assay, respectively. As shown in Fig. 4a, free DOX had poor selectivity between tumor and normal cells, so there was not too much difference in its cytotoxicities against HepG2 cell line (IC_{50} 1.03 ± 0.13 μM) and L-O2 cell line (IC_{50} 0.44 ± 0.11 μM). The BP9a-SS-DOX conjugate exhibited impressed antiproliferative activity against HepG2 cells with an IC_{50} value of 6.21 ± 1.12 μM which was lower than that of free DOX. However, the cytotoxic effect of this conjugate on L-O2 cells was obviously reduced in comparison with that of free DOX (Fig. 4b), indicating that the specific cytotoxicity of DOX against liver cancer cells is tremendously improved by coupling with TfR targeted binding peptide analog BP9a. Considering the cytotoxic effect on normal tissues is

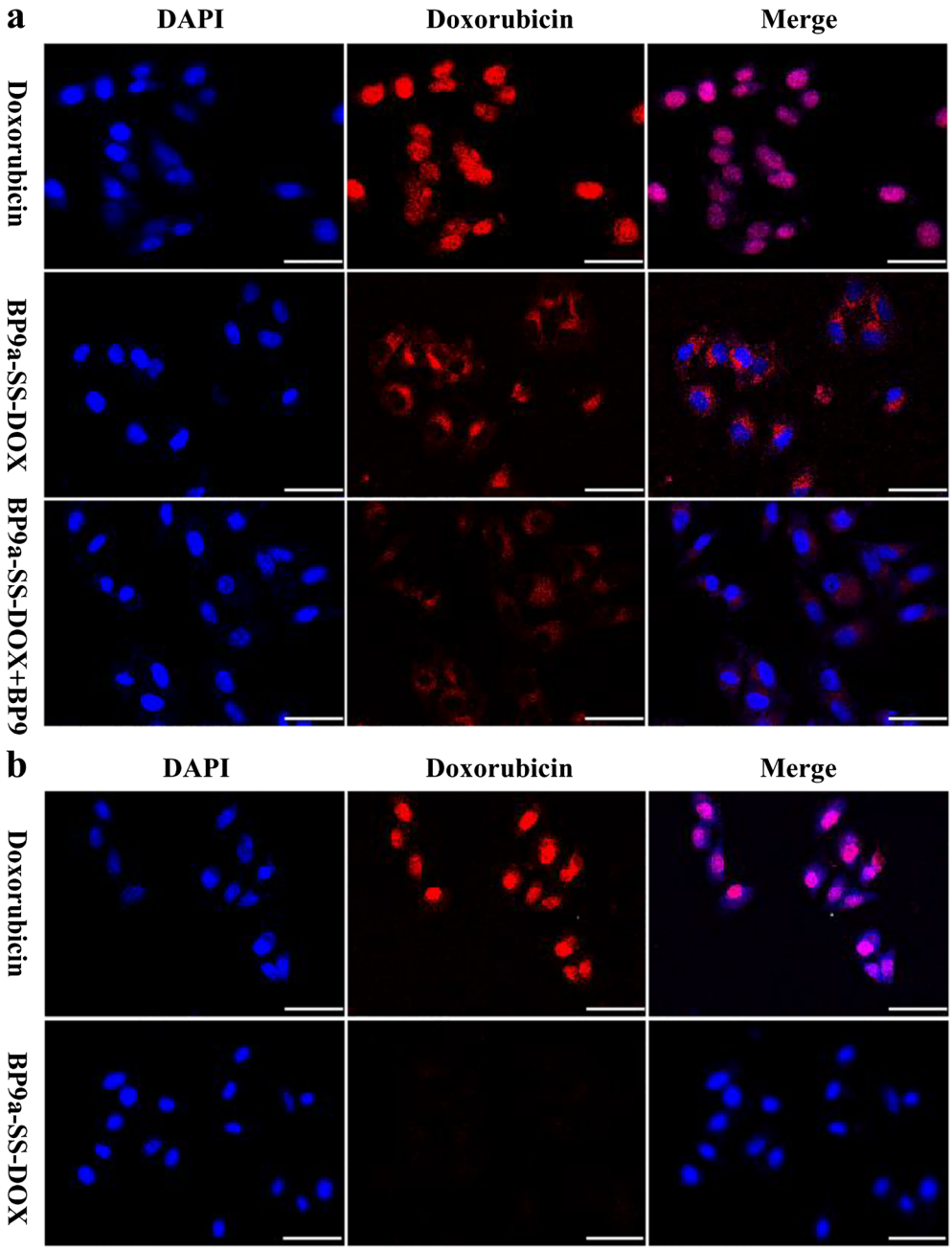

Fig. 3 Intracellular images of HepG2 (**a**) and L-O2 (**b**) cells after *in vitro* treatment with free DOX or the BP9a-SS-DOX conjugate for 3 h. For TfR competitive inhibition assay, HepG2 cells were preincubated with BP9 for 2 h and then treated with the BP9a-SS-DOX conjugate. Images from left to right show blue fluorescence in cell nuclei stained by DAPI, red fluorescence came from DOX, and pink color produced by merging the first two images. Scale bars = 75 μm.

the major drawback in the clinical application of DOX, the specific cytotoxicity of this peptide-doxorubicin conjugate against tumor cells is of significant importance. As illustrated in Fig. 5, the reason for the selective cytotoxicity of the BP9a-SS-DOX conjugate might be related to endocytosis mediated by the targeted binding of BP9a towards TfR overexpressed on the surface of HepG2 cells, the intramolecular disulfide bond between BP9a and DOX was cleaved under the reductive condition (higher GSH concentration) within tumor cells, so DOX-SH can be efficiently released from the conjugate to kill the tumor cells. While for L-O2 cells, which express low level of TfR, the entry of the BP9a-SS-DOX conjugate into cells was clearly decreased compared with that of HepG2 cells. Even though a small number of the conjugates could enter

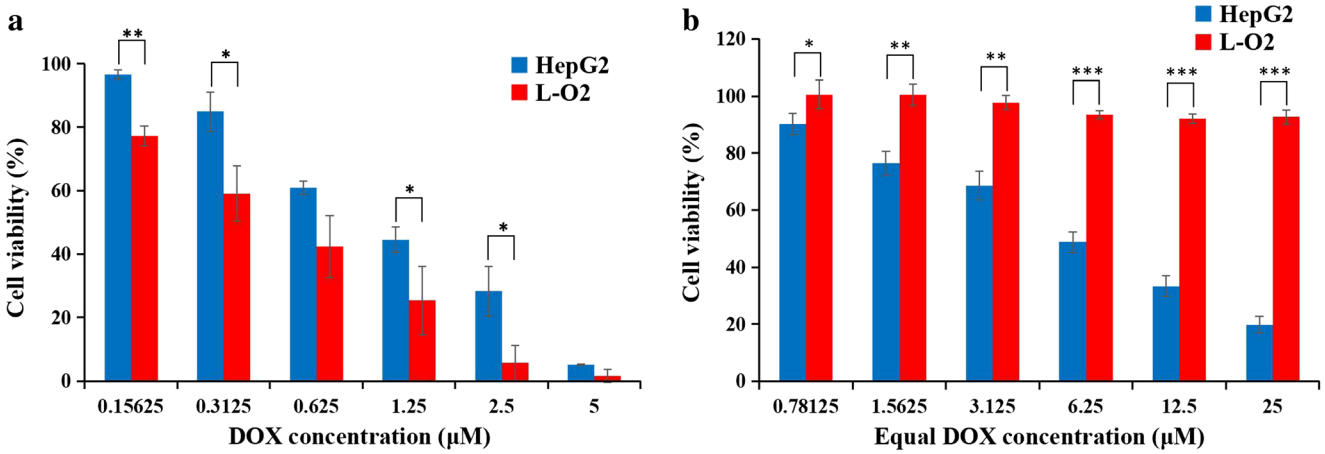

Fig. 4 The cytotoxic effects of free DOX (**a**) and the BP9a-SS-DOX conjugate (**b**) on HepG2 and L-O2 cells after 48 h incubation. Evaluations were performed using CCK-8 assay and cell viability was expressed as percentage of untreated controls (100%). Data were presented as mean ± standard deviation ($n = 3$); *$p < 0.05$, **$p < 0.01$, ***$p < 0.001$.

into cells, the intramolecular disulfide bond would be relatively stable in the very low GSH condition within normal cells, and DOX-SH was not able to be released from the conjugate as it did in the HepG2 cells, therefore exerting low cytotoxicity.

Although the present BP9a-SS-DOX conjugate showed good selectivity to tumor cells, its antitumor potency was lower than that of free DOX, which was possibly due to release of DOX-SH but not free DOX within tumor cells. DOX bioconjugates containing intramolecular hydrazone bond can be cleaved under the acidic intracellular condition and efficiently release free DOX. In order to improve the antiproliferative efficacy of DOX that was connected with BP9a, synthesis of conjugate with intramolecular

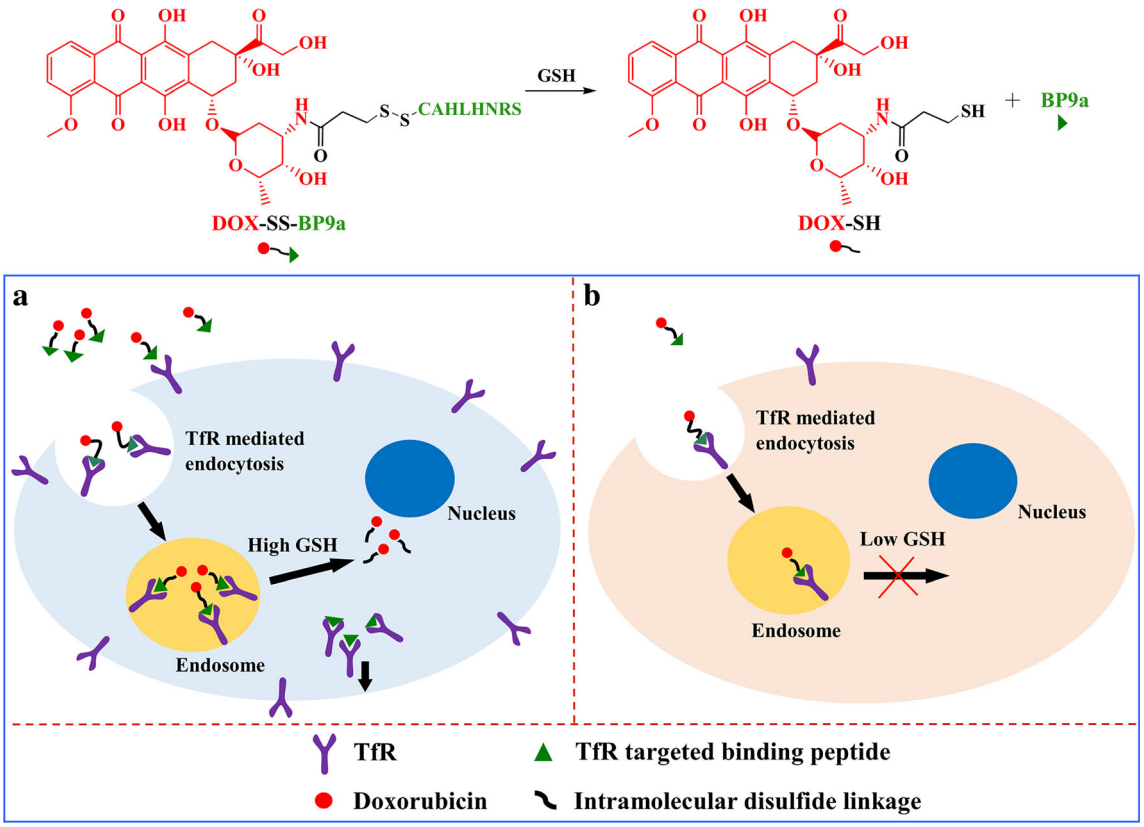

Fig. 5 Schematic illustration of the entry pathway, cellular uptake and drug release of the BP9a-SS-DOX conjugate in HepG2 (**a**) and L-O2 (**b**) cells.

hydrazone bond linkage and the targeted antitumor activity experiments will be implemented in the near future.

CONCLUSION

In summary, a novel TfR targeted and reduction-responsive peptide-drug conjugate (BP9a-SS-DOX) was successfully synthesized according to our design. The BP9a-SS-DOX conjugate showed a TfR mediated entry pathway into HepG2 liver cancer cells over-expressing TfR and rapidly collapse to release DOX-SH into cytoplasm under the reductive microenvironment within tumor cells. The antiproliferative activity of this peptide-drug conjugate against HepG2 cells was lower than that of free DOX, but its cytotoxic effect on L-O2 hepatic cells expressing low level of TfR was significantly reduced in comparison with that of free DOX. Therefore, it exhibited specific cytotoxicity against tumor cells. Our results suggest that the TfR binding peptide analog BP9a has the potential to be used as a promising peptide carrier for selective drug delivery.

ACKNOWLEDGMENTS AND DISCLOSURES

We acknowledge the Natural Science Foundation of Hebei Province (grant number H2017406022), the Scientific Research Projects of Hebei Province Education Department (grant number BJ2017055, ZD2016061 and ZD2017003), the Natural Science Research Project of Chengde Medical University (grant number 201915) and the Key Discipline Construction Projects of Hebei Province Higher School ([2013]4) for financial support of this work. The authors would like to thank Institute of Basic Medicine at Chengde Medical University for support during the bio-activity study.

REFERENCES

1. Majumdar S, Siahaan TJ. Peptide-mediated targeted drug delivery. Med Res Rev. 2012;32(3):637–58.
2. Pérez-Herrero E, Fernández-Medarde A. Advanced targeted therapies in cancer: drug nanocarriers, the future of chemotherapy. Eur J Pharm Biopharm. 2015;93:52–79.
3. Böhme D, Beck-Sickinger AG. Drug delivery and release systems for targeted tumor therapy. J Pept Sci. 2015;21(3):186–200.
4. Gilad Y, Firer M, Gellerman G. Recent innovations in peptide based targeted drug delivery to cancer cells. Biomedicines. 2016;4(2):11.
5. Kundu A, Nayak DP. Analysis of the signals for polarized transport of influenza virus (a/WSN/33) neuraminidase and human transferrin receptor, type II transmembrane proteins. J Virol. 1994;68(3):1812–8.
6. Lambert LA, Mitchell SL. Molecular evolution of the transferrin receptor/glutamate carboxy-peptidase II family. J Mol Evol. 2007;64(1):113–28.
7. Neckers LM, Trepel JB. Transferrin receptor expression and the control of cell growth. Cancer Investig. 1986;4(5):461–70.
8. Han L, Huang RQ, Liu SH, Huang SX, Jiang C. Peptide-conjugated PAMAM for targeted doxorubicin delivery to transferrin receptor overexpressed tumors. Mol Pharm. 2010;7(6):2156–65.
9. Daniels TR, Bernabeu E, Rodríguez JA, Patel S, Kozman M, Chiappetta DA, *et al.* The transferrin receptor and the targeted delivery of therapeutic agents against cancer. Biochim Biophys Acta-General Subjects. 2012;1820(3):291–317.
10. Tortorella S, Karagiannis TC. The significance of transferrin receptors in oncology: the development of functional nano-based drug delivery systems. Curr Drug Deliv. 2014;11(4):427–43.
11. Jeong SM, Hwang S, Seong RH. Transferrin receptor regulates pancreatic cancer growth by modulating mitochondrial respiration and ROS generation. Biochem Biophys Res Commun. 2016;471(3):373–9.
12. Nogueira-Librelotto DR, Codevilla CF, Farooqi A, Rolim CMB. Transferrin-conjugated nanocarriers as active-targeted drug delivery platforms for cancer therapy. Curr Pharm Des. 2017;23(3):454–66.
13. Li XR, Yang L, Yang Y, Shao M, Liu Y. Preparation and characterization of a novel monoclonal antibody against the extracellular domain of human transferrin receptor. Monoclon Antib Immunodiagn Immunother. 2017;36(1):1–7.
14. Chiu RYT, Tsuji T, Wang SJ, Wang J, Liu CT, Kamei DT. Improving the systemic drug delivery efficacy of nanoparticles using a transferrin variant for targeting. J Control Release. 2014;180:33–41.
15. Kang T, Jiang MY, Jiang D, Feng XY, Yao JH, Song QX, *et al.* Enhancing glioblastoma-specific penetration by functionalization of nanoparticles with an iron-mimic peptide targeting transferrin/transferrin receptor complex. Mol Pharm. 2015;12(8):2947–61.
16. Amin HH, Meghani NM, Park C, Nguyen VH, Tran TT, Tran PH, *et al.* Fattigation-platform nanoparticles using apo-transferrin stearic acid as a core for receptor-oriented cancer targeting. Colloids Surf B Biointerfaces. 2017;159:571–9.
17. Yoon DJ, Chen KY, Lopes AM, Pan AA, Shiloach J, Mason AB, *et al.* Mathematical modeling of mutant transferrin-CRM107 molecular conjugates for cancer therapy. J Theor Biol. 2017;416:88–98.
18. Lin X, Yan SZ, Qi SS, Xu Q, Han SS, Guo LY, *et al.* Transferrin-modified nanoparticles for photodynamic therapy enhance the antitumor efficacy of hypocrellin A. Front Pharmacol. 2017;8:815.
19. Jhaveri A, Deshpande P, Pattni B, Torchilin V. Transferrin-targeted, resveratrol-loaded liposomes for the treatment of glioblastoma. J Control Release. 2018;277:89–101.
20. Deshpande P, Jhaveri A, Pattni B, Biswas S, Torchilin V. Transferrin and octaarginine modified dual-functional liposomes with improved cancer cell targeting and enhanced intracellular delivery for the treatment of ovarian cancer. Drug Deliv. 2018;25(1):517–32.
21. Dai Y, Huan JC, Xiang B, Zhu HL, He C. Antiproliferative and apoptosis triggering potential of paclitaxel-based targeted-lipid nanoparticles with enhanced cellular internalization by transferrin receptors-a study in leukemia cells. Nanoscale Res Lett. 2018;13(1):271.
22. Zhang L, Zhu XY, Wu SJ, Chen YZ, Tan SM, Liu YJ, *et al.* Fabrication and evaluation of a γ-PGA-based self-assembly transferrin receptor-targeting anticancer drug carrier. Int J Nanomedicine. 2018;13:7873–89.
23. Muddineti OS, Kumari P, Ghosh B, Biswas S. Transferrin-modified vitamin-E/lipid based polymeric micelles for improved

tumor targeting and anticancer effect of curcumin. Pharm Res. 2018;35(5):97.
24. Tang JJ, Wang QT, Yu QW, Qiu Y, Mei L, Wan DD, *et al.* A stabilized retro-inverso peptide ligand of transferrin receptor for enhanced liposome-based hepatocellular carcinoma-targeted drug delivery. Acta Biomater. 2019;83:379–89.
25. Tortorella S, Karagiannis TC. Transferrin receptor-mediated endocytosis: a useful target for cancer therapy. J Membr Biol. 2014;247:291–307.
26. Yang JD, Yang QY, Xu L, Lou J, Dong Z. An epirubicin-peptide conjugate with anticancer activity is dependent upon the expression level of the surface transferrin receptor. Mol Med Rep. 2017;15(1):323–30.
27. Mukherjee B, Karmakar SD, Hossain CM, Bhattacharya S. Peptides, proteins and peptide/protein-polymer conjugates as drug delivery system. Protein Pept Lett. 2014;21(11):1121–8.
28. Saw PE, Song EW. Phage display screening of therapeutic peptide for cancer targeting and therapy. Protein Cell. 2019. https://doi.org/10.1007/s13238-019-0639-7.
29. Wu CH, Liu IJ, Lu RM, Wu HC. Advancement and applications of peptide phage display technology in biomedical science. J Biomed Sci. 2016;23(1):8.
30. Dai XY, Xiong YL, Xu DD, Li LY, Su ZJ, Zhang QH, *et al.* TfR binding peptide screened by phage display technology-characterization to target cancer cells. Trop J Pharm Res. 2014;13(3):331–8.
31. Zheng Q, Xiong YL, Su JZ, Zhang QH, Dai XY, Li LY, *et al.* Expression of curcin–transferrin receptor binding peptide fusion protein and its anti-tumor activity. Protein Expr Purif. 2013;89(2):181–8.
32. Ducry L, Stump B. Antibody-drug conjugates: linking cytotoxic payloads to monoclonal antibodies. Bioconjug Chem. 2010;21(1):5–13.
33. Hu W, Cheng L, Cheng LF, Zheng M, Lei QF, Hu ZY, et al. Redox and pH-responsive poly (amidoamine) dendrimer-poly(ethylene glycol) conjugates with disulfide linkages for efficient intracellular drug release. Colloids Surf B Biointerfaces. 2014;123:254–63.
34. Kuppusamy P, Li HQ, Ilangovan G, Cardounel AJ, Zweier JL, Yamada K, et al. Noninvasive imaging of tumor redox status and its modification by tissue glutathione levels. Cancer Res. 2002;62:307–12.
35. Dong HQ, Tang M, Li Y, Li YY, Qian D, Shi DL. Disulfide-bridged cleavable PEGylation in polymeric nanomedicine for controlled therapeutic delivery. Nanomedicine. 2015;10(12):1941–58.
36. Fan ML, Yang DB, Liang XF, Ao JP, Li ZH, Wang HY, *et al.* Design and biological activity of epidermal growth factor receptor-targeted peptide doxorubicin conjugate. Biomed Pharmacother. 2015;70:268–73.
37. Lelle M, Kaloyanova S, Freidel C, Theodoropoulou M, Musheev M, Niehrs C, *et al.* Octreotide-mediated tumor-targeted drug delivery via a cleavable doxorubicin-peptide conjugate. Mol Pharm. 2015;12(12):4290–300.
38. Song Q, Chuan XX, Chen BL, He B, Zhang H, Dai WB, *et al.* A smart tumor targeting peptide-drug conjugate, pHLIP-SS-DOX: synthesis and cellular uptake on MCF-7 and MCF-7/Adr cells. Drug Deliv. 2016;23(5):1734–46.
39. Burns KE, Delehanty JB. Cellular delivery of doxorubicin mediated by disulfide reduction of a peptide-dendrimer bioconjugate. Int J Pharm. 2018;545(1–2):64–73.
40. Li ST, Zhao HL, Yin ZF, Deng SH, Chang AQ, Qi L. Synthesis of hepatoma transferrin receptor targeting peptide analogue BP9a. Chemistry & Bioengineering. 2018;35(12):27–9.
41. Yoon S, Kim WJ, Yoo HS. Dual-responsive breakdown of nanostructures with high doxorubicin payload for apoptotic anticancer therapy. Small. 2013;9(2):284–93.
42. Du X, Xiong L, Dai S, Qiao SZ. γ-PGA-coated mesoporous silica nanoparticles with covalently attached prodrugs for enhanced cellular uptake and intracellular GSH-responsive release. Adv Healthc Mater. 2015;4(5):771–81.
43. Shi NQ, Gao W, Xiang B, Qi XR. Enhancing cellular uptake of activable cell-penetrating peptide-doxorubicin conjugate by enzymatic cleavage. Int J Nanomedicine. 2012;7:1613–21.
44. Yang YF, Yang Y, Xie XY, Cai XS, Zhang H, Gong W, *et al.* PEGylated liposomes with NGR ligand and heat-activable cell-penetrating peptide–doxorubicin conjugate for tumor-specific therapy. Biomaterials. 2014;35(14):4368–81.
45. Ye WL, Du JB, Zhang BL, Na R, Song YF, Mei QB, *et al.* Cellular uptake and antitumor activity of DOX-hyd-PEG-FA nanoparticles. PLoS One. 2014;9(5):e97358.
46. Sheng Y, Xu JH, You YW, Xu FF, Chen Y. Acid-sensitive peptide-conjugated doxorubicin mediates the lysosomal pathway of apoptosis and reverses drug resistance in breast Cancer. Mol Pharm. 2015;12(7):2217–28.
47. Scomparin A, Salmaso S, Eldar-Boock A, Ben-Shushan D, Ferber S, Tiram G, *et al.* A comparative study of folate receptor-targeted doxorubicin delivery systems: dosing regimens and therapeutic index. J Control Release. 2015;208:106–20.
48. Ai SB, Duan JL, Liu X, Bock S, Tian Y, Huang ZB. Biological evaluation of a novel doxorubicin-peptide conjugate for targeted delivery to EGF receptor-overexpressing tumor cells. Mol Pharm. 2011;8(2):375–86.
49. Nasrolahi Shirazi A, Tiwari R, Chhikara BS, Mandal D, Parang K. Design and biological evaluation of cell-penetrating peptide-doxorubicin conjugates as prodrugs. Mol Pharm. 2013;10(2):488–99.
50. Soudy R, Chen C, Kaur K. Novel peptide-doxorubicin conjugates for targeting breast cancer cells including the multidrug resistant cells. J Med Chem. 2013;56(19):7564–73.